

3D Printing of Non-iridescent Structural Color Inks for Optical Anti-counterfeiting

Qilin Guo, Xiuli Wang, Dr. Jia Guo, Dr. Changchun Wang*

State Key Laboratory of Molecular Engineering of Polymers, Department of Macromolecular Science and Laboratory of Advanced Materials, Fudan University, Shanghai 200433, China

* Corresponding author: C. C. Wang, E-mail: ccwang@fudan.edu.cn

This text includes three supplementary tables show experimental materials, Characterization methods, size characteristics of obtained SiO₂, SiO₂@PDA and SiO₂@PDA@PHEMA nanoparticles, supplementary Fig. 1-14.

Calculation of the average refractive index of SiO₂@PDA particles

Generally, the average refractive index of hybrid nanoparticles can be calculated using the following equation (1):

$$n_m^2 = \sum n_i^2 V_i \quad (1)$$

in which n_m , n_i , V_i represents average refractive index of hybrid nanoparticles, refractive index and volume fraction of SiO₂ or PDA, respectively. The volume fraction of SiO₂ or PDA particles can be calculated by diameters or thickness measured by TEM images. For example, the diameter of SiO₂ core is 171 nm and the thickness of PDA shell is 9 nm in SiO₂@PDA with 189 nm, which can be achieved that V_{silica} is 81.9% and V_{PDA} is 18.1%. Therefore, the average refractive index (n_m) of SiO₂@PDA is 1.51.

Experimental Section

Materials: Tetraethyl orthosilicate (TEOS, 99%), tris(hydroxymethyl) aminomethane (Tris) and dopamine hydrochloride (DA·HCL) were obtained from Shanghai Aladdin Chemistry Co., Ltd. L-arginine (99%) was purchased from Energy-Chemical Co., Ltd. Hydroxyethyl methacrylate (HEMA, 99%), acrylic acid (AA), methacrylic acid (MAA), Hydroxyethyl acrylate (HEA), Hydroxybutyl acrylate (4-HBA), acetonitrile (ACN) and aqueous ammonia solution ($\text{NH}_3\cdot\text{H}_2\text{O}$, 25%) were purchased from Shanghai Chemical Reagents Company (China) and used as received. 2,2-azobis (isobutyronitrile) (AIBN) and N, N'-methylenebis-(acrylamide) (MBA) were all purchased from Shanghai Aladdin Chemistry Co. Ltd. (China) and AIBN was recrystallized from ethanol for three times. Deionized water and anhydrous ethanol (95%) were used in all experiments.

Characterization methods: Dynamic light scattering instrument (DLS, Malvern Zetasizer Nano ZS90) was used to record the hydrodynamic particle size, distribution of nanoparticles and Zeta potentials under a helium-neon laser light source, which should be noted that the particle size is slightly larger than that by TEM due to the swollen state in water. Transmission electron microscopy (TEM, Tecnai G2 20 TWIN, FEI) was used to characterized nanoparticles' size at an operating voltage of 200 kV. Field emission scanning electron microscopy (FESEM) micrographs were collected with a Zeiss Ultra 55 operated at a 3 kV and a working distance of 5.0-8.0 mm. The well-prepared samples were coated with Au at 10 mA for 120 s using a spray coater before measurement. Portable fiber spectrometer (Ideaoptics PG2000-Pro) was used to carry out the reflective spectra, and the standard aluminum mirror (100% reflection) was used as a reference. Photographs were taken illuminated with a LED light source against a dark background using a smartphone. Modular rheometer platform (Haake MARS III, Thermofisher) was used to analyze the MNCs rheological properties at 300 K using a plate–plate geometry with a 0.85 mm gap size, including storage modulus (G'), loss modulus (G'') and viscosity (η). The printing patterns were fabricated using a 3D printing system (3D Bio-Architect workstation, Regenovo Biotechnology).

Tables:

Table S1. Characteristic of SiO₂@PDA nanoparticles with the same core of SiO₂ (171nm).

Sample code	TEM-ave. (nm) ^a	Z-ave. (nm) ^b	PDI	Zeta potential (mV) ^b
Blue	180	192	0.082	-43.6
Green-1	189	208	0.046	-45.1
Yellow-1	195	232	0.081	-41.9
Orange	208	265	0.034	-43.8

^a Particle diameters measured from TEM images; ^b Results from DLS measured reports.

Table S2. Characteristic of core SiO₂ nanoparticles.

Sample code	TEM-ave. (nm) ^a	Z-ave. (nm) ^b	PDI	Zeta potential (mV) ^b
SiO ₂ -1	165	175	0.063	-43.4
SiO ₂ -2	182	196	0.092	-46.6
SiO ₂ -3	201	213	0.044	-43.9
SiO ₂ -4	223	232	0.068	-46.9

^a Particle diameters measured from TEM images; ^b Results from DLS measured reports.

Table S3. Characteristic of SiO₂@PDA nanoparticles with corresponding cores of SiO₂ in Table S2.

Sample code	TEM-ave. (nm) ^a	Z-ave. (nm) ^b	PDI	Zeta potential (mV) ^b
Violet	176	230	0.078	-50.1
Cyan	209	263	0.053	-51.2
Green-2	232	284	0.021	-49.9
Yellow-2	255	322	0.033	-48.7

^a Particle diameters measured from TEM images; ^b Results from DLS measured reports.

Figures:

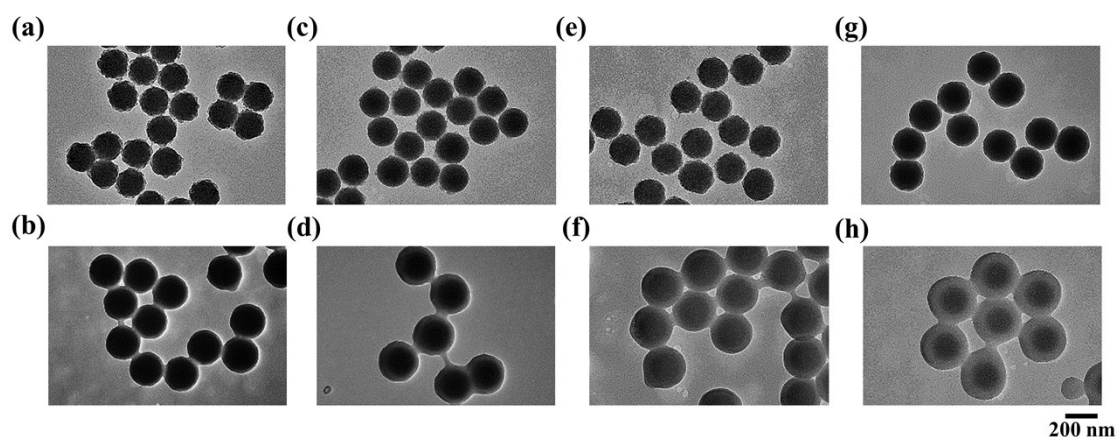


Fig. S1. TEM images of $\text{SiO}_2@PDA$ nanoparticles with diameters of (a) 180 nm, (c) 189 nm, (e) 195 nm and (g) 208 nm, respectively; and $\text{SiO}_2@PDA@PHEMA$ nanoparticles with diameters of (b) 204 nm, (d) 222 nm, (f) 264 nm and (h) 310 nm, respectively.

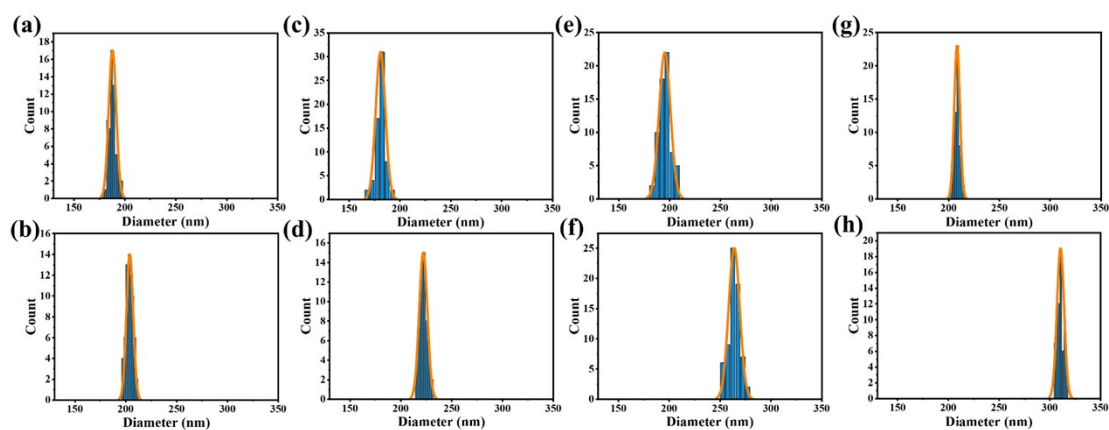


Fig. S2. The diameter distribution histograms of $\text{SiO}_2@PDA$ nanoparticles with diameters of (a) 180 nm, (c) 189 nm, (e) 195 nm and (g) 208 nm, respectively; and $\text{SiO}_2@PDA@PHEMA$ nanoparticles with diameters of (b) 204 nm, (d) 222 nm, (f) 264 nm and (h) 310 nm, respectively.

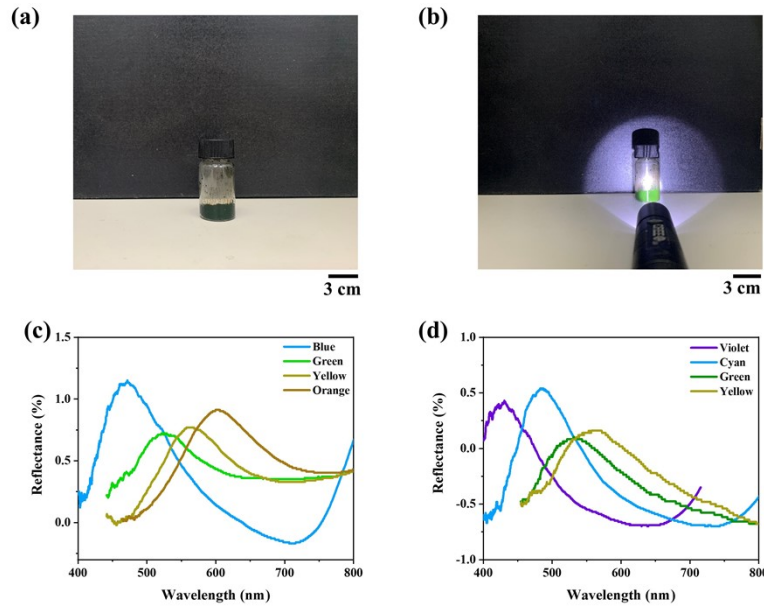


Fig. S3. Photographs of green structural color inks formed by $\text{SiO}_2@\text{PDA}@\text{PHEMA}$ nanoparticles with 291 nm under (a) ambient illumination and spot illumination by a flashlight with strong light source that has the luminous intensity of 107~114 Lumens. (c) The reflection spectra of structural color inks with $\text{SiO}_2@\text{PDA}@\text{PHEMA}$ nanoparticles with diameters of 204 nm, 222 nm, 264 nm and 310 nm, respectively. (d) The reflection spectra of structural color inks with $\text{SiO}_2@\text{PDA}@\text{PHEMA}$ nanoparticles with diameters of 213 nm, 262 nm, 291 nm and 308 nm, respectively.

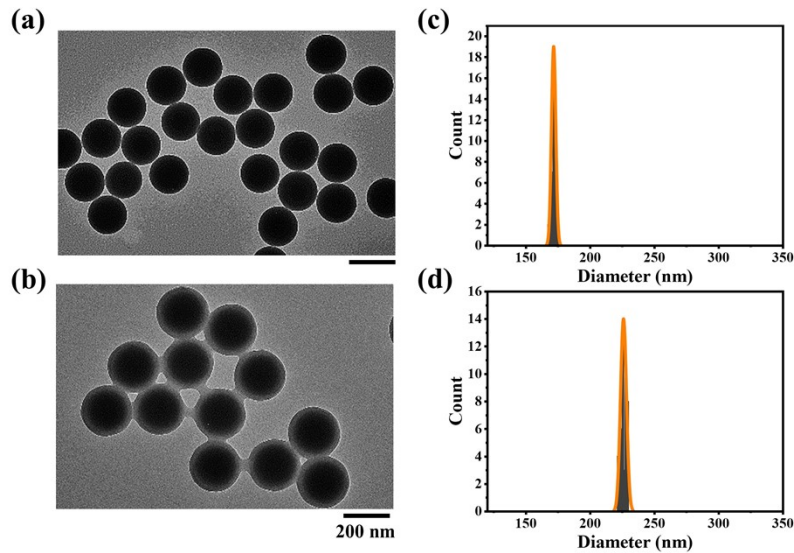


Fig. S4. TEM images of SiO_2 nanoparticles with diameters of (a) 171 nm and (c) the corresponding diameter distribution histograms. TEM images of $\text{SiO}_2@\text{PHEMA}$ nanoparticles with diameters of (b) 226 nm and (d) the corresponding diameter distribution histograms.

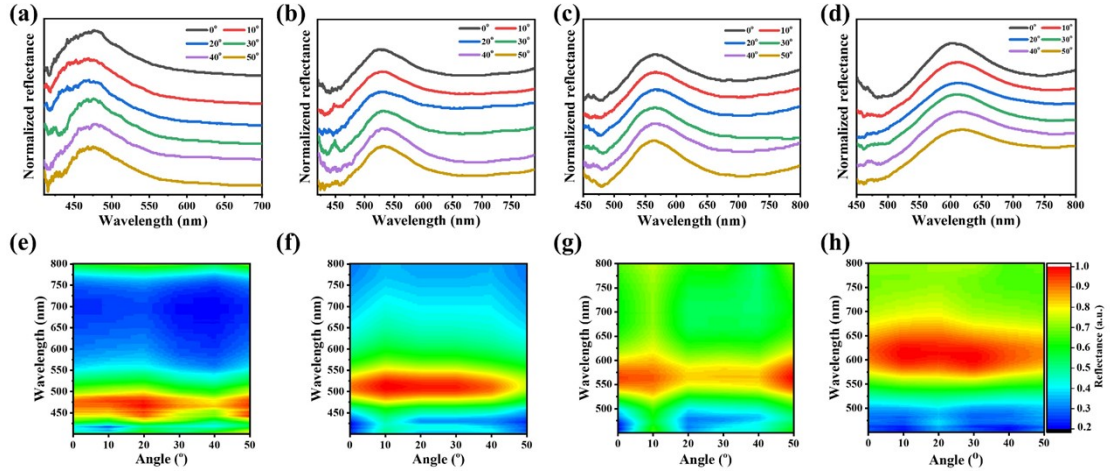


Fig. S5. Reflection spectra of the photonic inks formed by $\text{SiO}_2@\text{PDA}@\text{PHEMA}$ at various detection angles: (a) 204 nm, (b) 222 nm, (c) 264 nm and (d) 310 nm, respectively. The corresponding reflection contour spectra with different diameters of $\text{SiO}_2@\text{PDA}@\text{PHEMA}$ of (e) 204 nm, (f) 222 nm, (g) 264 nm and (h) 310 nm, respectively.

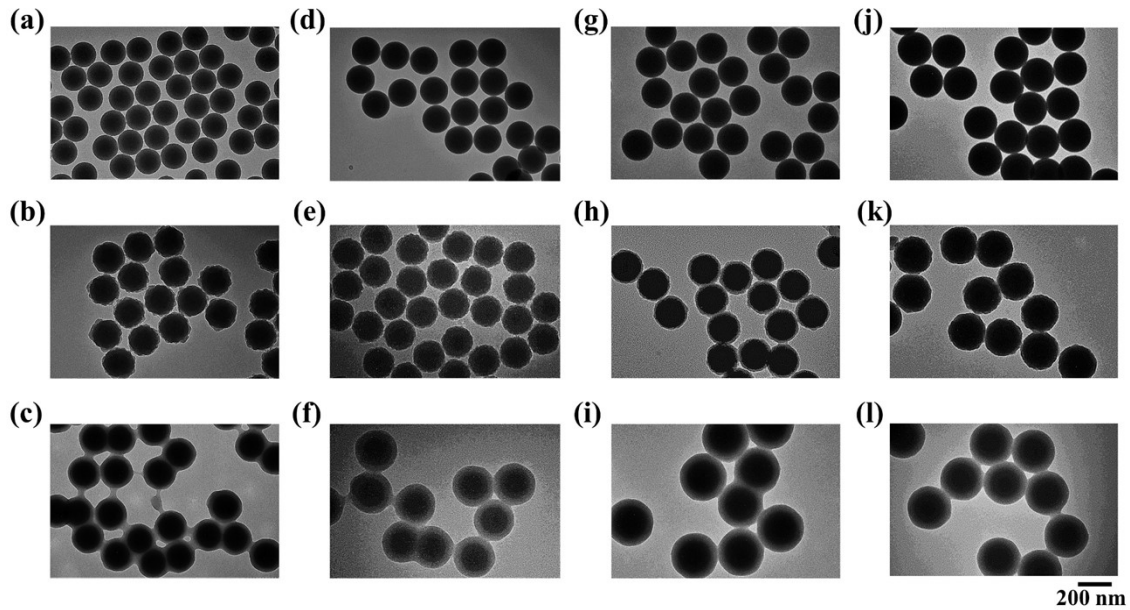


Fig. S6. TEM images of SiO_2 nanoparticles with diameters of (a) 165 nm, (d) 182 nm, (g) 201 nm and (j) 223 nm, respectively; $\text{SiO}_2@\text{PDA}$ nanoparticles with diameters of (b) 176 nm, (e) 209 nm, (h) 232 nm and (k) 255 nm, respectively; and $\text{SiO}_2@\text{PDA}@\text{PHEMA}$ nanoparticles with diameters of (c) 213 nm, (f) 262 nm, (i) 291 nm and (l) 308 nm, respectively.

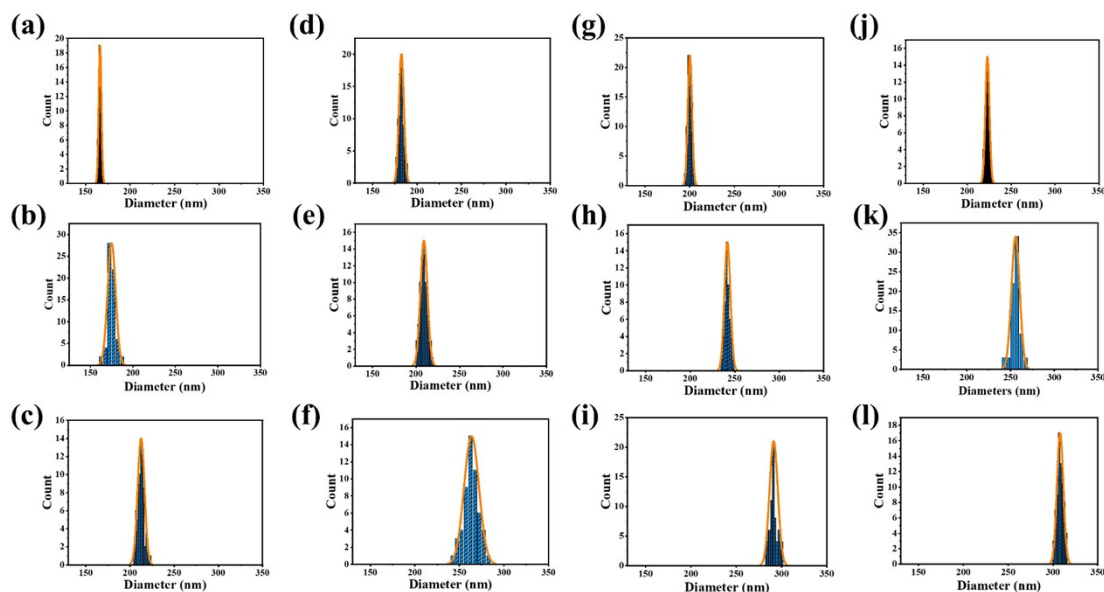


Fig. S7. The diameter distribution histograms of SiO₂ nanoparticles with diameters of (a) 165 nm, (d) 182 nm, (g) 201 nm and (j) 223 nm, respectively; SiO₂@PDA nanoparticles with diameters of (b) 176 nm, (e) 209 nm, (h) 232 nm and (k) 255 nm, respectively; and SiO₂@PDA@PHEMA nanoparticles with diameters of (c) 213 nm, (f) 262 nm, (i) 291 nm and (l) 308 nm, respectively.

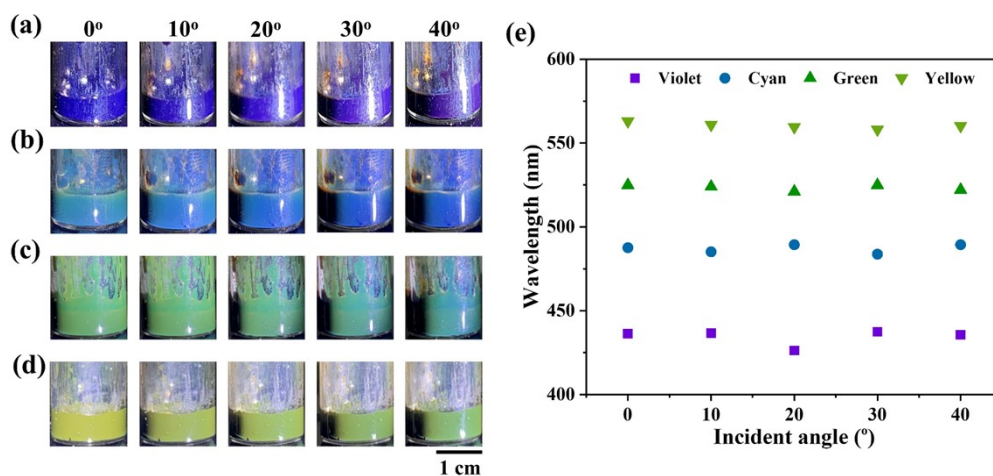


Fig. S8. Digital photographs of the structural color inks formed by SiO₂@PDA@PHEMA nanoparticles with different sizes of (a) 213 nm, (b) 262 nm, (c) 291 nm and (d) 308 nm, respectively, showing no obvious iridescent at various viewing angles. (e) The changing of maximum reflection wavelength of the photonic inks at different detection angles from 0° to 40°.

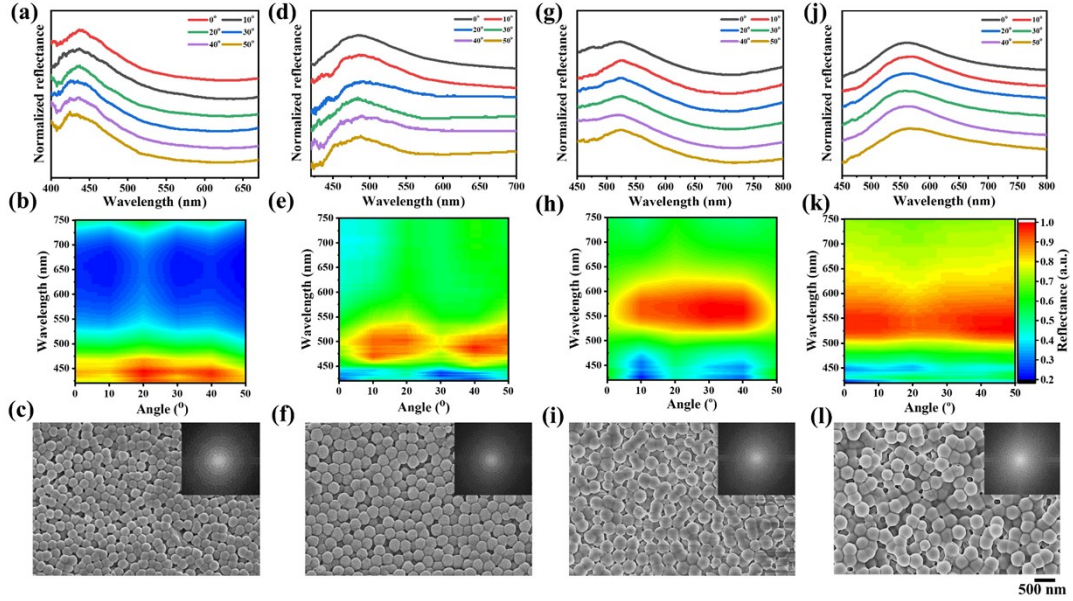


Fig. S9. Reflection spectra of the photonic inks with different sizes of $\text{SiO}_2@\text{PDA}@\text{PHEMA}$ at various detection angles: (a) 213 nm, (d) 262 nm, (g) 291 nm and (j) 308 nm, respectively. The corresponding reflection contour spectra with different sizes of $\text{SiO}_2@\text{PDA}@\text{PHEMA}$ of (b) 213 nm, (e) 262 nm, (h) 291 nm and (k) 308 nm, respectively. SEM images and 2D fast Fourier transform (FFT) diagrams of non-iridescent photonic inks formed by different $\text{SiO}_2@\text{PDA}@\text{PHEMA}$ with size of (c) 213 nm, (f) 262 nm, (i) 291 nm and (l) 308 nm, respectively.

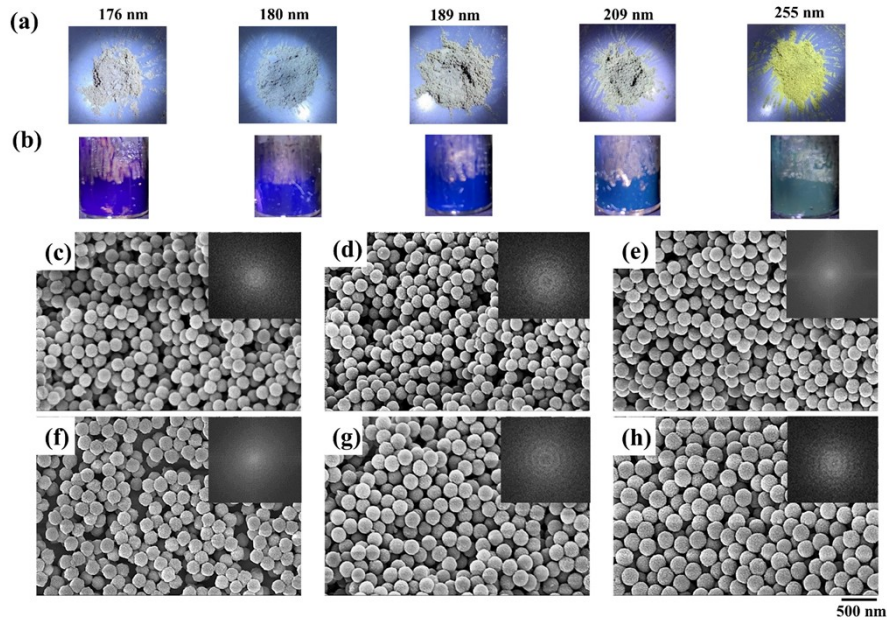


Fig. S10. (a) Powders and (b) photonic inks consisted of $\text{SiO}_2@\text{PDA}$ at various diameters of 176 nm, 180 nm, 189 nm, 209 nm and 255 nm, respectively. SEM images and 2D fast Fourier transform (FFT) diagrams of non-iridescent photonic inks formed by different $\text{SiO}_2@\text{PDA}$ with the size of (c) 176 nm, (d) 180 nm, (e) 189 nm, (f) 209 nm, (g) 245 nm and (h) 255 nm, respectively.

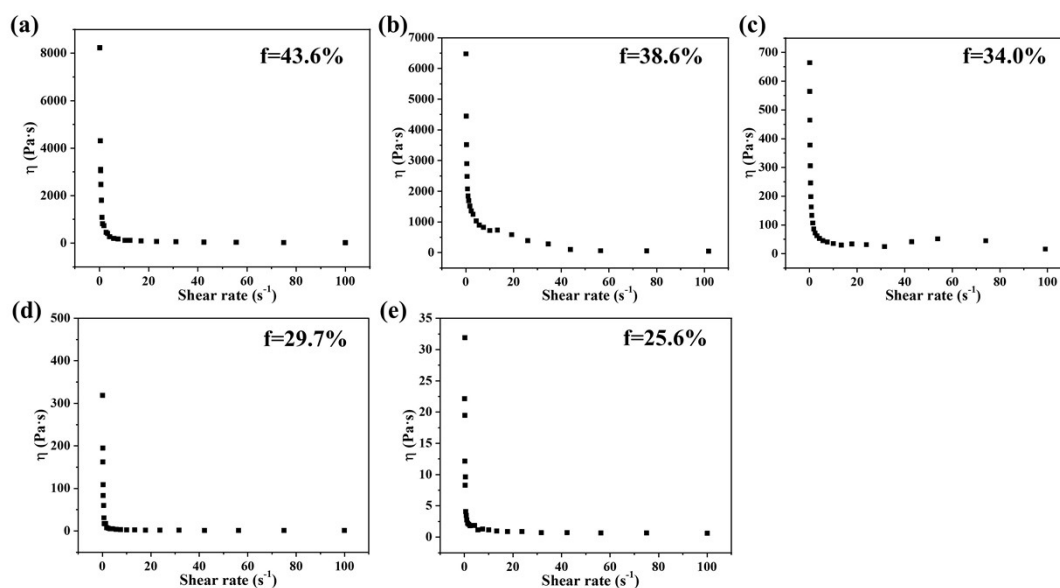


Fig. S11. The photonic inks viscosity of HEMA mixed with $\text{SiO}_2\text{@PDA@PHEMA}$, in which the volume fraction of (a) 43.6%, (b) $f=38.6\%$, (c) $f=34.0\%$, (d) $f=29.7\%$ and (e) $f=25.6\%$, respectively.

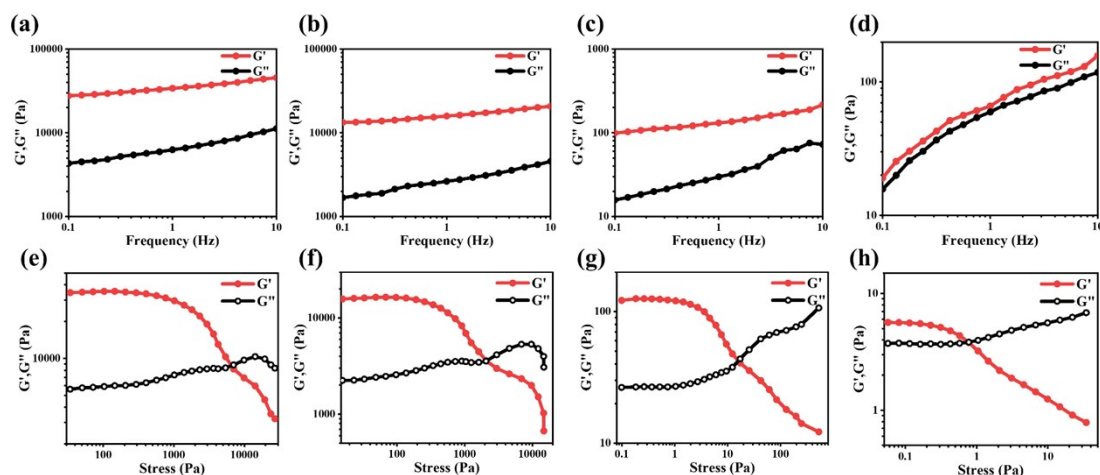


Fig. S12. The storage modulus (G') and loss modulus (G'') of the photonic inks including $\text{SiO}_2\text{@PDA@PHEMA}$ nanoparticles with 291 nm at the volume fraction of (a) 43.6%, (b) $f=38.6\%$, (c) $f=29.7\%$ and (d) $f=25.6\%$ as a function of oscillatory frequency, respectively. The corresponding changes of G' and G'' of inks containing particles at the volume fraction of (e) 43.6%, (f) $f=38.6\%$, (g) $f=29.7\%$ and (h) $f=25.6\%$ as a function of increased shear stress, respectively.

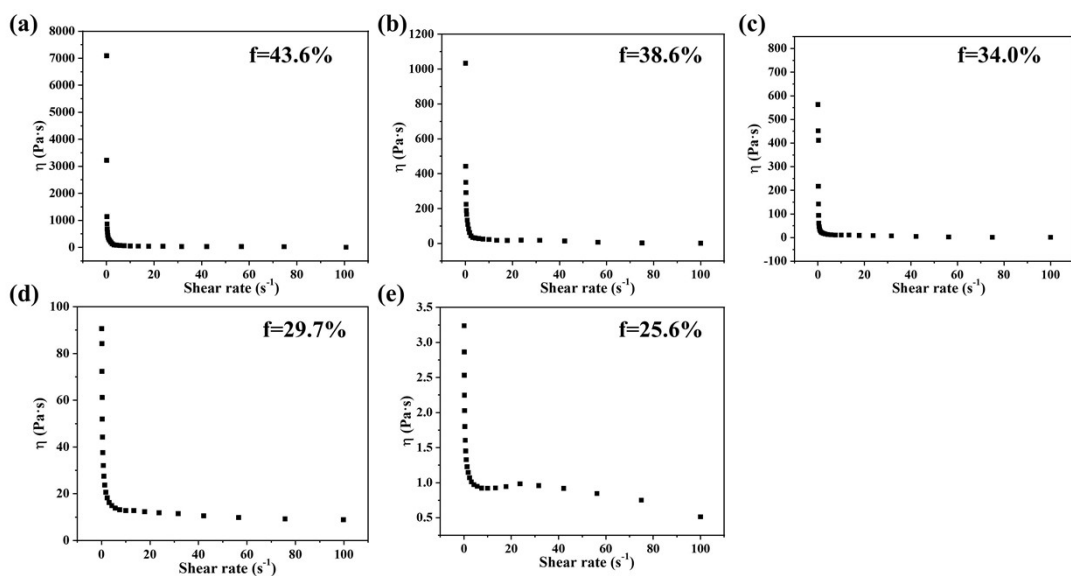


Fig. S13. The inks viscosity of HEMA mixed with $\text{SiO}_2\text{@PDA}$, where the volume fraction of (a) 43.6%, (b) $f=38.6\%$, (c) $f=34.0\%$, (d) $f=29.7\%$ and (e) $f=25.6\%$, respectively.

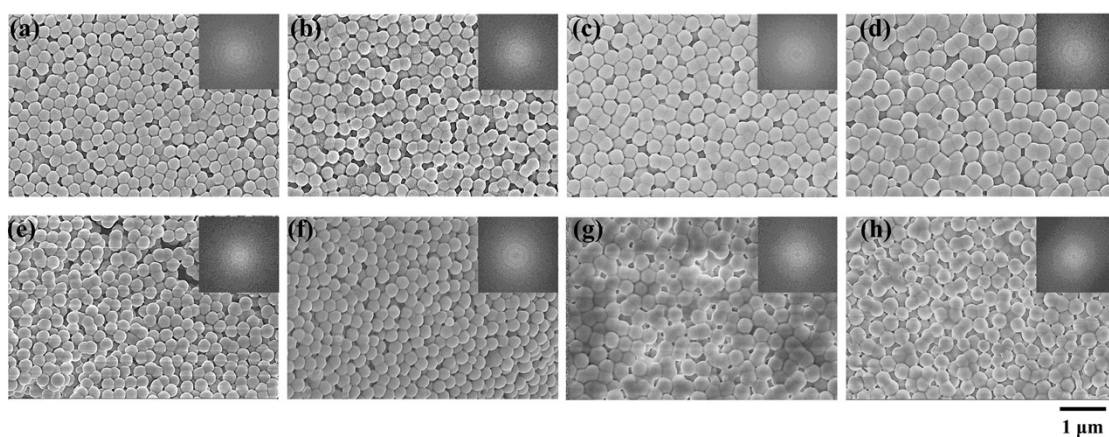


Fig. S14. SEM images and 2D fast Fourier transform (FFT) diagrams of surface of printed patterns with different diameters of $\text{SiO}_2\text{@PDA@PHEMA}$ of (a) 204 nm, (b) 222 nm, (c) 264 nm, (d) 310 nm, (e) 213 nm, (f) 262 nm, (g) 291 nm and (h) 308 nm, respectively.